Investigation of the early stages in laser-induced ignition by Schlieren photography and laser-induced fluorescence spectroscopy

M. Lackner, S. Charareh, and F. Winter

Institute of Chemical Engineering, Vienna University of Technology, Getreidemarkt 9/166, A-1060 Wien, Austria
lackner@mail.zserv.tuwien.ac.at , fwinter@mail.zserv.tuwien.ac.at

K. F. Iskra, D. Rüdisser, and T. Neger

Institut für Experimentalphysik, TU Graz, Petersgasse 16, A-8010 Graz, Austria
iskra@tugraz.at , neger@tugraz.at

H. Kopecek and E. Wintner

Institute of Photonics, Vienna University of Technology, Gußhausstraße 25-29, A-1040 Wien, Austria
hkopece@pop.tuwien.ac.at , ewintner@pop.tuwien.ac.at

Abstract: Laser ignition has been discussed widely as a potentially superior ignition source for technical appliances such as internal combustion engines. Ignition strongly affects overall combustion, and its early stages in particular have strong implications on subsequent pollutant formation, flame quenching, and extinction. Our research here is devoted to the experimental investigation of the early stages of laser-induced ignition of CH_4/air mixtures up to high pressures. Tests were performed in a 0.9-l combustion cell with initial pressures of up to 25 bar with stoichiometric to fuel-lean mixtures using a 5-ns 50-mJ 1064-nm Nd:YAG laser. Laser-induced fluorescence (LIF) was used to obtain two dimensionally resolved images of the OH radical distribution after the ignition event. These images were used to produce an animation of laser ignition and early flame kernel development. Schlieren photography was used to investigate the laser-induced shock wave, hot core gas, and developing flame ball. We extend existing knowledge to high-pressure regimes relevant for internal combustion engines.

OCIS codes: (280.1740) Combustion diagnostics; (300.2530) Spectroscopy, Fluorescence, laser-induced; (999.9999) Laser ignition, laser-induced ignition

References and Links

1. H. Kopecek, E. Wintner, H. Pischinger, G. Herdin, and J. Klausner, "Basics for a future laser ignition system for gas engines," ICE-Vol.**35**-2, Paper No. 2000-ICE-316, 2000 ICE Fall Technical Conference ASME 2000, Peoria USA (2000).
2. T. X. Phuoc, "Single-point versus multi-point laser ignition: experimental measurements of combustion times and pressures," Combustion and Flame **122**, 508-510 (2000).
3. M. H. Morsy, Y. S. Ko, S. H. Chung, and P. Cho, "Laser-induced two-point ignition of premixture with a single-shot laser," Combust. Flame **125**, 724-727 (2001).
4. J. X. Ma, T. W. R. Ill, and J. P. Buckingham, "Nd:YAG laser ignition of natural gas," Paper 98-ICE-114, ICE Vol. **30**-3, Spring Technical Conference ASME (1998).
5. J. X. Ma, D. R. Alexander, and D. E. Poulain, "Laser spark ignition and combustion characteristics of methane-air mixtures," Combust. Flame **112**, 492-506 (1998).

#4518 - $15.00 US Received 2 June 2004; revised 19 August 2004; accepted 13 September 2004

6. H. Kopecek, M. Lackner, E. Wintner, F. Winter, and A. Hultqvist, "Laser-stimulated ignition in a homogeneous charge compression ignition engine, SAE paper 2004-01-0937, 2004 SAE World Congress, Detroit, USA, March 8–11 (2004).
7. J. D. Dale, M. D. Checkel, and P. R. Smy, "Application of high energy ignition systems to engines," Prog. Energy Combust. Sci. **23**, 379-398 (1997).
8. T. X. Phuoc, "Laser spark ignition: experimental determination of laser-induced breakdown thresholds of combustion gases," Opt. Commun. **175**, 419-423 (2000).
9. H. Kopecek, M. Lackner, F. Winter, and E. Wintner, "Laser ignition of methane-air mixtures at pressures up to 4 MPa," J. Laser Phys. **13**, 1365 (2003).
10. T.-W. Lee, V. Jain, and S. Kozola, "Measurements of minimum ignition energy by using laser sparks for hydrocarbon fuels in air: propane, dodecane, and jet-a fuel," Combust. Flame **125**, 1320-1328 (2001).
11. R. Hickling and W. R. Smith, "Combustion tests of laser ignition," SAE paper 740114, Society of Automotive Engineers (1974).
12. J. D. Dale, P. R. Smy, and R. M. Clements, "Laser ignited internal combustion engine—an experimental study," SAE paper 780329, Society of Automotive Engineers (1978).
13. G. S. Settles, *Schlieren and Shadowgraph Techniques* (Springer, 2001).
14. S. Cheskis, "Quantitative measurements of absolute concentrations of intermediate species in flames," Progress in Energy and Combustion Science **25** (3), 233-252 (1999).
15. H. Östmark, M. Carlson, and K. Ekvall, "Concentration and temperature measurements in a laser-induced high explosive ignition zone. Part I: LIF spectroscopy measurements," Combust. Flame **105** (3), 381-390 (1996).
16. Y. L. Chen, J. W. L. Lewis, and C. Parigger, "Probability distribution of laser-induced breakdown and ignition of ammonia," Journal of Quantitative Spectroscopy and Radiative Transfer. 66(1), 41-53 (2000).
17. M. Villagran-Muniz, H. Sobral, and R. Navarro-Gonzalez, "Shock and thermal wave study of laser-induced plasmas in air by the probe beam deflection technique," Measurement Science and Technology **14**, 614-618 (2003).
18. Z. Liu, G. J. Steckman, and D. Psaltis, "Holographic recording of fast phenomena," Appl. Phys. Lett. **80**(5), 731-733 (2002).
19. J.-L. Beduneau, B. Kim, L. Zimmer, and Y. Ikeda, "Measurements of minimum ignition energy in premixed laminar methane/air flow by using laser induced spark," Combust. Flame **132**, 653-665 (2003).
20. R. Navarro-Gonzalez and M. Villagran-Muniz, "Effect of beam waist on shock properties of laser-induced plasmas in air by the photoacoustic probe beam deflection method," Analytical Sciences **17**, 118-121 (2001).
21. N. Lamoureux, N. Djebaili-Chaumeix, and C.-E. Paillard, "Laminar flame velocity determination for H_2-airHe-CO_2 mixtures using spherical bomb method," Experimental Thermal and Fluid Science **27**(4), 385-393 (2003).
22. Y. Ra and W. K. Cheng, "Laminar flame propagation through a step-stratified charge," The Fifth International Symposium on Diagnostics and Modeling of Combustion in Internal Combustion Engines (COMODIA 2001), Nagoya, Japan (2001).
23. T. A. Spiglanin, A. Mcilroy, E. W. Fournier, R. B. Cohen, and J. A. Syage, "Time-resolved imaging of flame kernels: laser spark ignition of H_2/O_2/Ar mixtures," Combust. Flame **102**:310-328 (1995).
24. R. W. Schmieder, "Laser spark ignition and extinction of a methane-air diffusion flame," J. Appl. Phys. **52**, 3000 (1981).
25. J. A. Syage, E. W. Fournier, R. Rianda, and R. B. Cohen, "Dynamics of flame propagation using laser-induced spark initiation: Ignition energy measurements," J. Appl. Phys. **64**, 1499 (1988).
26. W. Gretler and R. Regenfelder, "Similarity solution for laser-driven shock waves in a particle-laden gas," Fluid Dynamics Research **28**, 369-382 (2001).
27. Q. Qin, and K. Attenborough, "Characteristics and application of laser-generated acoustic shock waves in air," Appl. Acoust. **65**(4), 325-340 (2004).
28. Y.-L. Chen and J. W. Lewis, "Visualization of laser-induced breakdown and ignition," Opt. Express **9**, 360-371 (2001), http://www.opticsexpress.org/abstract.cfm?URI=OPEX-9-7-360.
29. H. Malm, G. Sparr, J. Hult, and C. F. Kaminski, "Nonlinear diffusion filtering of images obtained by planar laser-induced fluorescence spectroscopy," J. Opt. Soc. Am. A **17**, 2148-2156 (2000).

1. Introduction

Internal combustion engines play a dominant role in transportation and in energy production. The spark-ignited Otto engine has widespread use and has been the subject of continuous improvements. The ignition source, however, has remained comparatively unchanged in the past 100 years. An electrical spark plug essentially consists of two electrodes with a gap in

#4518 - $15.00 US Received 2 June 2004; revised 19 August 2004; accepted 13 September 2004

between where, upon application of a high voltage, an electrical breakdown occurs. By exchanging the electrically generated spark plug for a laser-generated one, provided that an industrially suitable laser source is available, one would have several advantages, among which are the free and optimum choice of ignition location. With large stationary engines, a prolonged lifetime would increase maintenance intervals and hence reduce costs [1]. For automobile applications, the costs of a laser ignition system would have to compete with those of the established spark-plug setup. Laser ignition was found to be capable of safely igniting leaner fuel/air mixtures than can be achieved with a spark plug. Lean burn operation results in reduced NO_x emissions and is therefore favorable. Lean mixtures have a reduced burning velocity; therefore multipoint ignition as studied in Refs. [2, 3] might eventually become necessary to compensate for the loss in flame speed for engine applications. The major obstacles in developing a future laser ignition system for engine use are high laser cost, laser reliability, sufficient pulse energy at high repetition rate [4], and optical window fouling [5].

Apart from laser spark ignition, laser-assisted auto ignition has also been investigated [6]. A review on alternative ignition systems such as laser ignition is presented in Ref. [7]. Laser ignition of gases, predominantly CH_4/air mixtures, has been studied previously [5, 8, 9] as well as laser ignition of liquid fuels [10]. Tests were performed both in static laboratory combustion cells [11] and in adapted engines [12]. Ignition is a complex phenomenon that strongly affects the subsequent combustion. The early stages in particular have strong implications on pollutant formation, flame propagation, and quenching. The time scale of a laser-induced spark is several orders of magnitude smaller than the time scales of turbulence and chemical kinetics. In Ref. [7] the importance of the spark time scale on flame kernel size and NO_x production is outlined. Our study focuses on the experimental investigation of the early stages of laser-induced ignition, which is the time span between the energy deposition by a focused laser beam (ns domain) to several tens of microseconds (detachment of the shock wave from the hot core air and outward propagation) to several milliseconds (development of the flame ball).

2. Experimental setup

The laser-induced ignition of stoichiometric to fuel-lean CH_4/air mixtures was studied experimentally in a thermostated constant-volume vessel (0.9 l) with temperatures ranging from 300 to 473 K and with initial pressures between 1 and 25 bar. The vessel is equipped with four windows made of sapphire. Two of them are opposite each other in the lateral and transverse direction (along the axis and perpendicular to it). A *Q*-switched Nd:YAG laser (Quantel Brilliant; 400 mJ, 1064 nm) is deployed for igniting the combustible mixture inside the vessel. The pulses (5-ns duration) can be attenuated by use of a two-step polarizer half-wave plate setup from 50 to 1 mJ. A pressure transducer in conjunction with a precision charge amplifier was used to determine the pressure inside the vessel. The stoichiometry of the air/CH_4 mixtures (the λ value) was determined by the partial pressures of the gases. Since CH_4 is a highly compressible gas, the exact λ was determined by gas chromatography. Details on the experimental setup can be found below in Fig. 1 and in Ref. [9].

2.1 Schlieren photography

To obtain information on media with refractive-index gradients, one can use either techniques relying on beam deflection such as Schlieren photography or shadowgraph or those using phase determination such as interferometry [17]. Another approach is given by photothermal methods, in particular, the probe-beam deflection technique [17]. Perpendicularly to the igniting laser beam, collimated light from a flash lamp (1-ms pulse duration) was directed through the combustion vessel. Because the index of refraction in gases is strongly dependent on the density, areas with gradients of temperatures or pressures have a considerable effect on

#4518 - $15.00 US Received 2 June 2004; revised 19 August 2004; accepted 13 September 2004

the propagation of light, and the refraction angle is proportional to the first derivate of these parameters [13]. The experimental setup for the Schlieren experiments is depicted in Fig. 1.

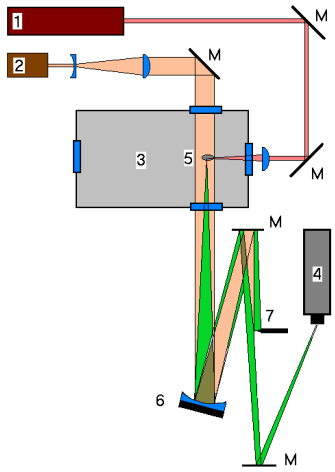

Fig. 1. Experimental setup for Schlieren photography; 1: pulsed Nd:YAG laser for ignition; 2: flash lamp; 3: combustion chamber; 4: CCD camera; 5: focus of the Nd:YAG laser beam; 6: spherical mirror (f = 660 mm); 7: knife edge or aperture; M: mirror.

The spherical mirror (6 in Fig. 1) has two functions: (1) It focuses the unscattered part of the incoming parallel light in the distance of its focal length f, and (2) it images a real and an inverted picture of the scattering area on the CCD chip of the camera. The magnification M of this image depends on the distance s from the Schlieren to the mirror and the distance s' from mirror to camera with the law for thin lenses: $\frac{1}{f} = \frac{1}{s} + \frac{1}{s'}$ and $M = \frac{s'}{s}$. Now the parallel part of the beam is cut out by placing an aperture in the focal region such that it covers the focused light but enables the scattered part to pass around the focal area.

The scattering direction depends on the direction of the diffraction-index gradient. If a razor edge is used as an aperture, which covers the whole focus region but allows the scattered light to pass only in the positive x direction from the focal point, the resulting picture will show the diffraction-index gradients only in the x direction. In our case a round aperture was used, since gradients in all directions were present, so that all the scattered light could pass. A high temporal resolution may be achieved by using either a fast light source or a fast camera. Here, a fast gateable intensified camera was chosen.

A major advantage in Schlieren photography is the uncomplicated setup. A disadvantage of the technique is that information from a volume is shown on a plane.

2.2 Laser-induced fluorescence

To gain additional information about the temporal and spatial characteristics of the flame kernel development in the first stages after ignition, a setup for recording of cross-sectional images via planar laser-induced fluorescence was employed. Laser-induced fluorescence (LIF) is a highly selective and sensitive method for detecting minor or transient species in chemical reacting flows, plasmas, or combustion processes. Excitation is performed by tuning a laser to a species-specific wavelength enabling a transition to an excited electronic state. Within the lifetime, the excited state decays by emitting light of wavelengths according to allowed transitions in the rotational–vibrational–electronic manifold. The signal is filtered, amplified. and, by expanding the scheme to a two-dimensional setup (planar LIF) with detection perpendicular to the excitation laser beam, provides information about the relative particle density distribution of the species under investigation. The setup is shown in Fig. 2.

#4518 - $15.00 US Received 2 June 2004; revised 19 August 2004; accepted 13 September 2004

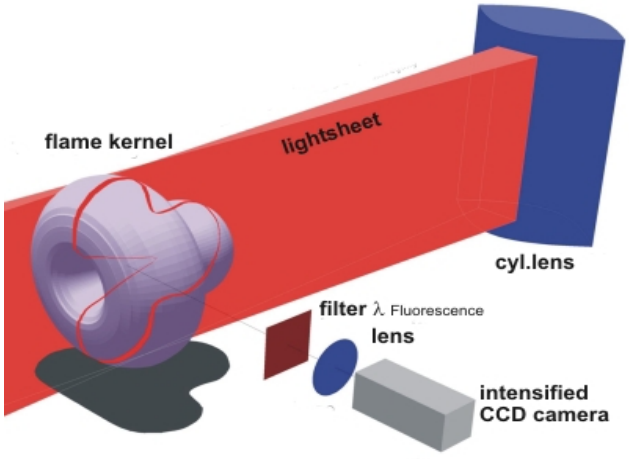

Fig. 2. Schematic setup for planar laser-induced fluorescence imaging.

Although the method is ideally suited for nonintrusive diagnostics in hostile environments, the drawback is the difficulty of obtaining reliable information about the absolute particle density. The major suppressing effect on the fluorescence signal is collisional quenching, i.e., radiationless removal of the excitation energy by collisions. The quenching rate is state specific, depends on the collision rate, and differs strongly between different colliders. The particle density of the colliders itself is mostly unknown, so for absolute concentration measurements without making too many assumptions about the chemical environment, one has to rely on methods based on linear absorption. But if only relative densities are sufficient for the information required, LIF or PLIF is the method of choice. In this case, PLIF was used to obtain temporally resolved two-dimensional cross sections of the early stage flame kernel development by use of the OH radical as a coarse flame front marker. Excitation was performed at the $A^2\Sigma(v'=1)$-$X^2\Pi(v''=0)$ Q_1 (J=6.5) transition at ~283 nm, which was chosen for its low temperature dependence under the expected experimental values. The detected fluorescence signal was selected by a 10-nm bandwidth interference filter centered at the $A^2\Sigma(v'=0)$-$X^2\Pi(v''=0)$ band at 310 nm. To minimize quenching effects, the gate of the intensified camera system was shifted as close as possible toward the time of the laser pulse. In Refs. [14–16], details of LIF applied to combustion and ignition diagnostics can be found.

3. Results and discussion

3.1 Schlieren photography

Schlieren photography was used to obtain visual information on the shock-wave formation and flame kernel development following the laser-induced breakdown and plasma formation. Images from the plasma emission show the typical asymmetric spark structure (domination of the inverse bremsstrahlung absorption process).

#4518 - $15.00 US Received 2 June 2004; revised 19 August 2004; accepted 13 September 2004

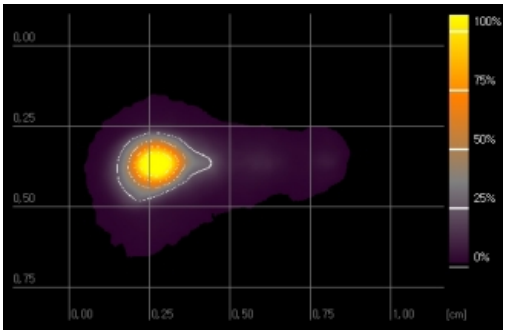

Fig. 3. Image of the emission 200 ns after breakdown in air. The ignition laser is entering from the left side. The asymmetric intensity results from the increased absorption of laser radiation by the generated plasma in the later stages of the pulse and has considerable effect on the ignition and flame propagation characteristics of laser-ignited gas mixtures. Experimental conditions: Pressure: 1 bar, medium: air, temperature: 300 K, exposure time: 3 ns, laser energy: 230 mJ.

Investigations on the plasma emission were performed in air at different pressures. The shape and structure of the emission zone is less dependent on the constituents, so these measurements were performed in air.

In a different investigation at 0.2 bar [17], a nearly perfect cylindrical shape whose size is of the order of the focal spot size was observed (domination by the multiphoton ionization process). In Ref. [17], the mechanisms leading to asymmetric flame kernel growth are discussed. Our observations confirm these findings at elevated pressures.

Breakdown leading to laser ignition is a process that is highly stochastic because of the nonlinear processes involved. In most experiments, only one breakdown in the focal region of the laser beam was observed. In Fig. 2 one can see the two shock waves break down at two locations. Note the effect of one shock wave on the propagation speed of the other. The interaction of two laser-induced shock waves is studied in Ref. [18].

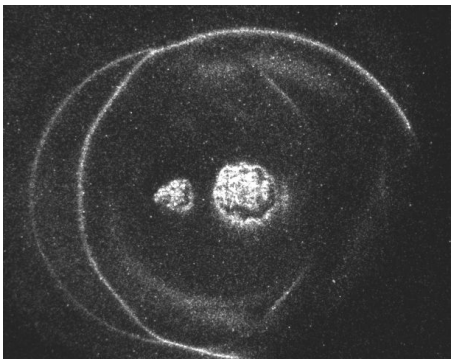

Fig. 4 Breakdown occurred at two locations simultaneously; therefore two shock waves can be observed. In the middle of these, one can see the hot core air. Less energy was deposited in the left region, so the resulting shock wave is smaller. Experimental conditions: Pressure: 25 bar, medium: air, temperature: 373 K, light source: flash lamp, exposure time: 30 ns, laser energy: 50 mJ, time: 8 μs after ignition; image dimensions: 11.6 mm × 9.15 mm.

#4518 - $15.00 US Received 2 June 2004; revised 19 August 2004; accepted 13 September 2004

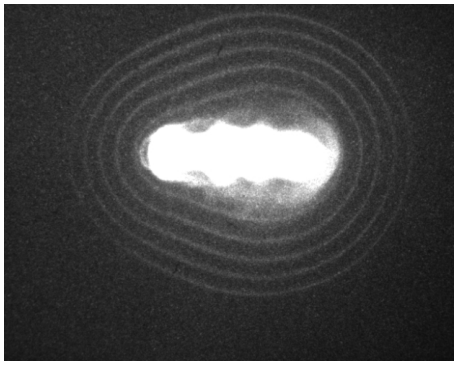

Fig. 5. Multiexposure image of the shock wave in air at 10 bar in 500-ns steps after ignition. The distance between the first two shock front structures outside the hot core gas is visibly larger than between the subsequent exposures. The imaging rate of the camera was at its fastest, so no exact shock-wave speed variation could be deduced from these multiexposure images.

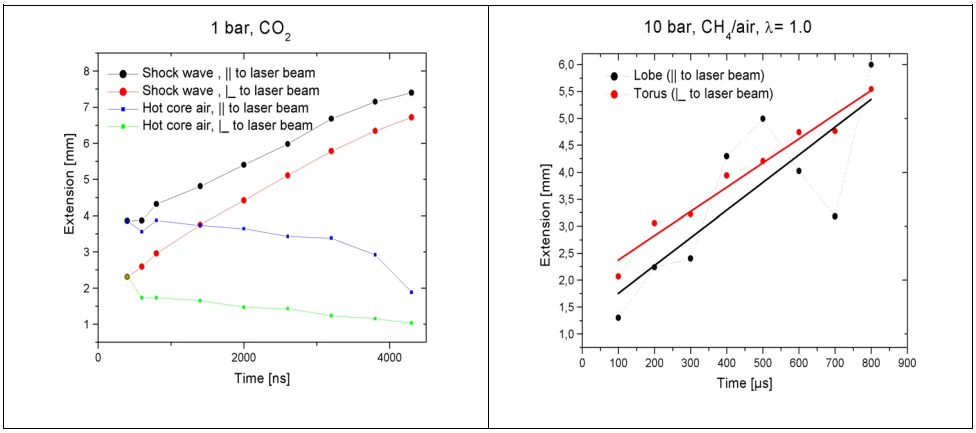

Fig. 6. Left: Dimensions of the shock wave and the hot core gas in 1 bar CO_2. Right: dimensions of the flame kernel in a stoichiometric CH_4/air mixture at 10 bar. ||: parallel direction to the igniting laser; |_: perpendicular to it.

The camera used had a repetition rate that allowed the recording of one image per ignition event, except for the multiexposure images obtainable in the shock-wave visualizations. All other multiexposures gave only blurry images. To study the temporal evolution of the ignition process, multiple images had to be recorded from multiple ignition events. Owing to the stochastic nature of the breakdown process, the initial size of the hot core air and shock wave varied considerably. Therefore, the images do not fit together perfectly (see Fig. 6, right). To obtain a semi-quantitative trend, however, the method was considered to be appropriate.

In Ref. [19], Schlieren images of CH_4/air mixtures in a laminar flow at 1 bar were obtained to study the flame kernel development and the shock-wave formation. The flame kernel dimensions and shock-wave expansion velocity were determined at 6 and 80 mJ. The air/fuel equivalence ratio λ was found to have a negligible influence on the size of the ellipsoidal kernel, but the spark energy was found to have a strong influence in that study.

3.1.1 Shock wave

The properties of the shock wave were investigated in air, CO_2, and H_2 at pressures between 1 and 25 bar. The shock wave has two major implications on laser ignition: First, it transports energy away from the ignition spot, and second, it causes a significant temperature rise. When

#4518 - $15.00 US Received 2 June 2004; revised 19 August 2004; accepted 13 September 2004

the shock wave has detached from the hot core air, both phenomena can be studied independently. The shock wave initially has an ellipsoidal shape caused by the asymmetric energy deposition of the laser. At a later stage, as it has propagated outward, the shock-wave front was found to approach a spherical geometry (see also Ref. [17]). Figure 7 shows the velocities of the shock wave in transverse direction to the igniting laser beam.

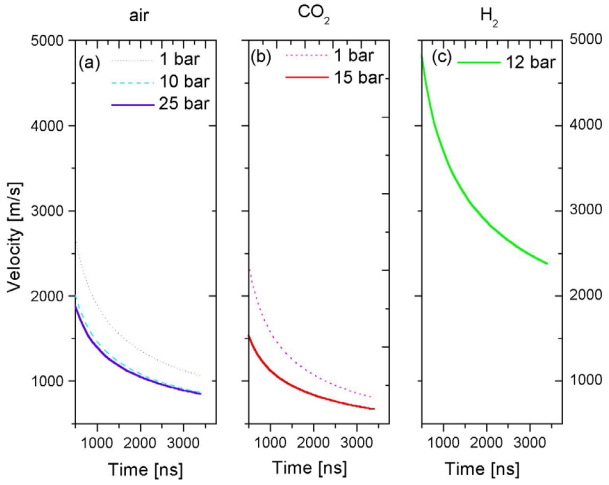

Fig. 7. Velocities of the shock waves in (a) air, (b) CO_2, and (c) H_2 at pressures between 1 and 25 bar. Note the same scales for all subfigures. The velocities were determined in the transverse direction to the igniting laser (torus).

In another study at 300-mJ pulse energy, the shock-wave velocity after 1 µs was found to be approximately 450 m/s in air at atmospheric pressure [17]. Here, we obtained roughly 1900 m/s for air at 1 bar after 1 µs. Since we could obtain only one image per ignition test, our uncertainty is rather large. As can be seen from Fig. 5, the shock-wave velocity decreases with pressure. As can be seen from the comparison of the shock-wave velocity in Figs. 5(a) and 5(c) for air and H_2, respectively, the shock-wave velocity also strongly depends on the composition. The shock-wave velocity was a function of the laser energy.

3.1.2 Hot core gas

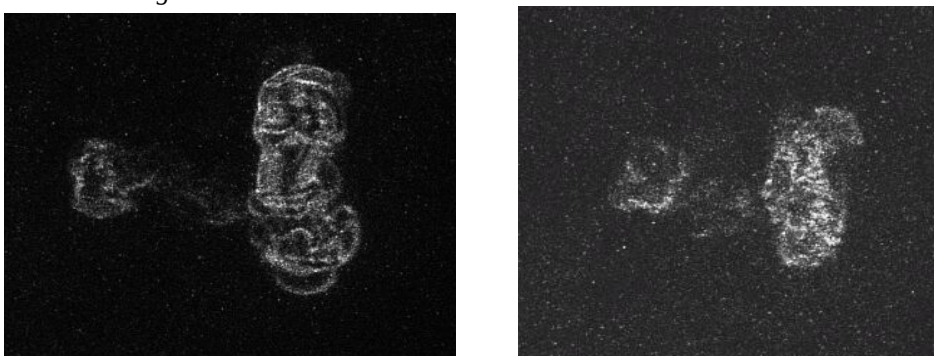

Fig. 8. Schlieren image of a stoichiometric CH_4/air mixture at 10 bar, 500 µs after ignition (left) and the corresponding image of the hot gas core in air (right) at identical conditions. The shock wave is far outside the region of observation; only the hot core of the gas mixture in the beginning stages of combustion is visible. The difference in size is not typical but can be attributed to variations of laser energy deposition. The structures in the combustible mixture are much sharper owing to the beginning of heat release and subsequent higher-density gradients in the flame front. Comparison with the corresponding image top right in Fig. 7 shows the OH-fluorescence signal in the same characteristical geometry.

#4518 - $15.00 US Received 2 June 2004; revised 19 August 2004; accepted 13 September 2004

The hot core gas (see Fig. 8, left) was studied in longitudinal and transverse direction to the igniting laser beam in air, CO_2, and H_2 at pressures between 1 and 25 bar. The relaxation time to bring the hot core gas back to room temperature was determined to be ~5 ms, which is in agreement with other results [17]. The expansion velocities of the hot core were determined to be approximately 40 and 4 m/s before and after the focus at ambient pressure in air. In our study, the extension of the hot core air was found to be between approximately 2 and 4 mm parallel to the laser beam and 1 and 2 mm in transverse direction immediately after the laser energy deposition. The decay rate upon shrinking obtained from the Schlieren was approximately 0.1–0.2 mm/µs.

3.1.3 Flame kernel

The properties of the developing flame kernel were investigated in CH_4/air mixtures at 10 bar at different air/fuel equivalence ratios of 1.0 and 1.5. In Fig. 9(a), one can see the extension of the hot core air in 10-bar air with time both in the longitudinal and the transverse directions. In Fig. 9(b), the growth of the flame kernel in a laser-ignited CH_4/air mixture at 10 bar is shown. As mentioned above, the data points exhibit a significant spread because only one picture could be taken during each test and the temporal evolution is in fact composed of a sequence of ignition tests. Nonetheless, one can see the trend quite well. The stoichiometric flame grows faster than the fuel-lean one, which is in agreement with the existing literature.

Within the scope of this study, it is not possible to extract the flame speed from the test data. In To obtain the laminar flame speed, one of the most important parameters of a combustible gas, Schlieren photography in a spherical bomb is a common method as outlined in Ref. [21] for diluted H_2/air mixtures. However, there are several major complications: The initial flame speed from laser ignition is higher than that of a flame initiated by spark-plug ignition [4]. This effect can be attributed to the turbulent motion of the hot core gas induced by the ignition laser plasma. The flame speed at early stages is strongly dependent on the laser energy but approaches equilibrium at later stages at approximately 10–20 ms. This effect is visible in the fluorescence images, although the view is restricted because of the small window diameter.

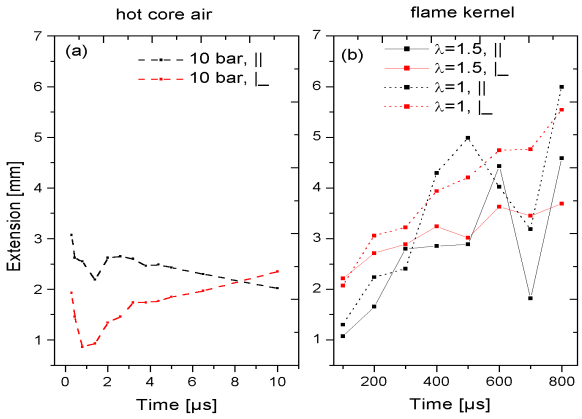

Fig. 9. Flame kernel in laser-ignited CH_4/air mixtures at 10 bar. (a) Temporal evolution of the hot core in air, (b) that of the flame kernel in a stoichiometric and fuel-lean CH_4/air mixture. Note that combustion is faster at $\lambda = 1$.

Also, one has to take into account that spherically expanding flames are subject to stretch in response to curvature and strain. The difference between the observed velocity and that of a plane flame is characterized by the Markenstein length [21]. Effects of excessive flame stretch have been observed in a separate investigation that uses formaldehyde instead of OH as a flame front marker. The results of that study are under evaluation.

#4518 - $15.00 US Received 2 June 2004; revised 19 August 2004; accepted 13 September 2004

3.2 Laser-induced fluorescence

In Ref. [28], Chen and Lewis used PLIF to investigate plasma kernel dynamics and flame development, which was identified as being essential for verifying modeling of laser ignition. In that study, investigations at higher pressures up to 25 bar were conducted.

The anisotropy of early flame kernel development is also evident in the images recorded by planar laser-induced fluorescence of the OH radical in the flame front. Because of the higher experimental effort and the limited recording rate, investigation of ignition parameters by sequential temporally shifted PLIF imaging was applied only to some selected sets of parameters in the case of CH_4-air mixtures. In a first step, the flame front was defined as the line of maximum signal after the first steep rise of the OH concentration. Three corresponding images were averaged, and a set of intermediate images were created by interpolation. The speed of the flame front was determined by the difference of two corresponding points defined by the direction of a vector in plane and orthogonal to the line determined previously. This gives a sequence of two-dimensional images corresponding to the flame development in the first few milliseconds after ignition. The three-dimensional structure can be assumed to be cylindrical symmetric. A set of images recorded perpendicular to the ignition laser and the symmetry of the images above and under the ignition laser direction proves this assumption. The set of images were combined into a movie showing the first toroidal expansion and a delayed but faster front-lobe formation typical of laser ignition in stationary media, which can be explained by the strong energy deposition on the laser-sided end of the breakdown plasma.

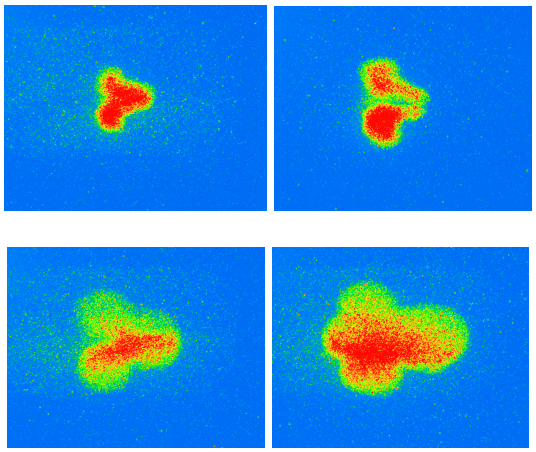

Fig. 10. Planar laser-induced fluorescence images of the OH radical, ignition laser entering from the right side. $\lambda = 1.0$; CH_4/air, 25 bar. Image diameter is 18 mm. From left to right: 0.2 , 0.5, 1.5, and 2.5 ms after ignition

#4518 - $15.00 US Received 2 June 2004; revised 19 August 2004; accepted 13 September 2004

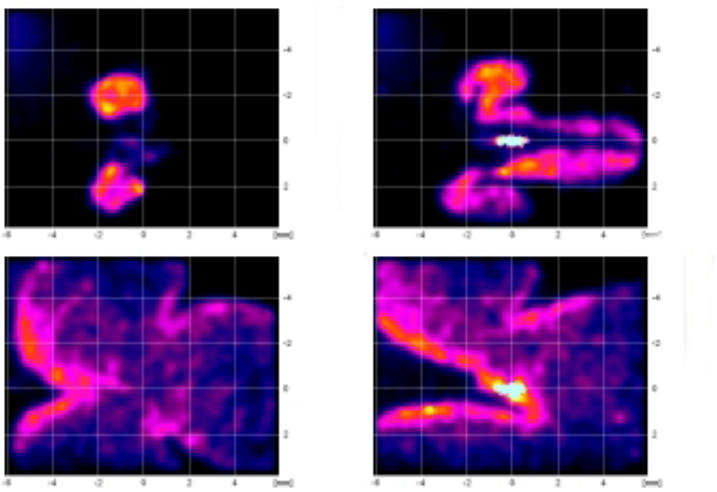

Fig. 11. Planar laser-induced fluorescence images of the OH radical, ignition laser entering from the right side. λ =1.3, CH_4/air 4.3 bar. Top row: 0.5 ms after ignition, from left to right: 50 mJ, 140 mJ ignition laser energy. Bottom row: 2.5 ms after ignition, from left to right: 50 mJ, 140 mJ ignition laser energy. Despite the difference in the first 500 µs after ignition the flame kernel geometry appears similar after 2.5 ms, showing the transition from turbulent to laminar flame front propagation. Observation of the full scale image was restricted by the window diameter.

The LIF images cover the same region as the Schlieren images, with some slight changes to account for focusing requirements with different optics. Figure 10 depicts OH LIF images obtained in a stoichiometric CH_4/air mixture at 25 bar. Figure 11 shows OH LIF images in a fuel-lean CH_4/air mixture at 4.3 bar. The geometry of the developing flame structure in these early stages after ignition is almost completely determined by the expansion and convection in response to the plasma kernel. At later stages—some 5 ms after ignition depending on pressure, composition, and laser energy—the structure smoothes visibly, and the flame speed approaches the laminar regime.

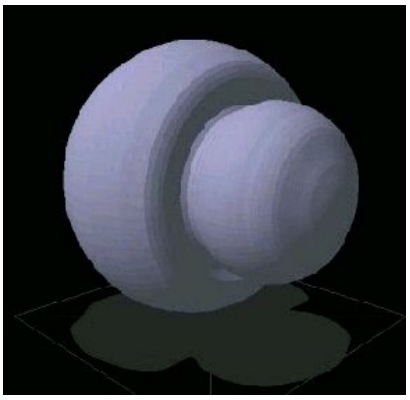

Fig. 12. (1.100 kB): Three-dimensional visualization of the flame front after laser ignition in a fuel-lean CH_4/air mixture.

In Fig. 12, a movie derived from OH PLIF data shows the flame kernel formation and propagation in a laser-ignited CH_4/air mixture at ambient pressure. Before evaluation, a separate set of PLIF-measurements perpendicular to the axis of ignition proved the degree of symmetry that allowed extrapolation of the data obtained in the plane of intersection to be

#4518 - $15.00 US Received 2 June 2004; revised 19 August 2004; accepted 13 September 2004

rotationally symmetric. For this particular set of data, a nonlinear fit algorithm for evaluation of PLIF data was used [29]. The literature contains a wealth of information on LIF studies of laser-induced ignition (e.g. Ref. [23]). Here, the flame front of the developing flame kernel was tracked by the OH radical to yield an animation, which we consider to be highly illustrative.

4. Summary

In this study, laser-induced ignition of gases was investigated experimentally. A Nd:YAG laser at 1064 nm was used for ignition. The early stages of combustion were investigated in CH_4/air mixtures at stoichiometric to fuel-lean conditions at ambient to elevated pressures. Results and trends reported in the literature, predominantly for the ambient pressure regime, could be verified up to high pressures.

Schlieren photography was used to study the laser-induced shock wave in H_2, CO_2, and air at initial pressures ranging from 1 to 25 bar. The shock wave velocity was determined to be approximately 1900 m/s at 1 bar in air after 1 µs. The shock-wave velocity is a function of the deposited laser energy. The dimension of the hot core air at the location of the laser plasma was determined to be approximately 2–4 mm parallel to the laser beam and 1–2 mm in transverse direction immediately after the laser energy deposition. The decay rate upon shrinking was approximately 0.1–0.2 mm/µs, being more or less independent of pressure.

Planar laser-induced fluorescence (PLIF) spectroscopy of the OH radical was used to learn about the plasma kernel dynamics and the flame development, which was identified as being essential for verifying the modeling of laser ignition. Here, studies at high pressures were conducted.

Acknowledgments

We thank Bernhard Schwecherl and Gabor Ast for assistance in the experiments. This research was supported by the Austrian Industrial Research Promotion Fund (FFF) under Grant FFF 803050 and by A3 project number 806238/7782. We gratefully acknowledge the fruitful industrial cooperation with G. Herdin and J. Klausner from GE Jenbacher GmbH & CO OHG.

#4518 - $15.00 US Received 2 June 2004; revised 19 August 2004; accepted 13 September 2004